JPE 12-2-10

http://dx.doi.org/10.6113/JPE.2012.12.2.317

Approximate Equivalent-Circuit Modeling and Analysis of Type-II Resonant Immittance Converters

Mangesh Borage†, K. V. Nagesh*, M. S. Bhatia*, and Sunil Tiwari**

†**Raja Ramanna Centre for Advanced Technology, Indore, India
*Bhabha Atomic Research Centre, Mumbai, India

Abstract

Resonant immittance converter (RIC) topologies can transform a current source into a voltage source (Type-I RICs) and vice versa (Type-II RICs), thereby making them suitable for many power electronics applications. RICs are operated at a fixed frequency where the resonant immittance network (RIN) exhibits immittance conversion characteristics. It is observed that the low-frequency response of Type-II RINs is relatively flat and that the state variables associated with Type-II RINs affect the response only at the high frequencies in the vicinity of the switching frequency. The overall response of a Type-II RIC is thus dominated by the filter response, which is particularly important for the controller design. Therefore, an approximate equivalent circuit model and a small-signal model of Type-II RICs are proposed in this paper, neglecting the high-frequency response of Type-II RINs. While the proposed models greatly simplify and speed-up the analysis, it adequately predicts the open-loop transient and small-signal ac behavior of Type-II RICs. The validity of the proposed models is confirmed by comparisons of their results with those obtained from a cycle-by-cycle simulation and with an experimental prototype.

Key words: Current supplies, Equivalent Circuit, Immittance Converters, Resonant power conversion, Soft-switching

I. INTRODUCTION

Resonant converters (RCs) have been a potential candidate in many power electronics applications involving high-frequency power processing such as dc-dc converters [1], high voltage power supplies [2], power factor correction [3], electronic lamp ballasts [4], induction heating [5], etc. The merits of RCs include soft switching, high frequency operation, high efficiency, small size, gainful utilization of the circuit parasitic components, etc. Some RCs also inherently have unique and useful characteristics that may not be exhibited by the other classes of power electronics converters.

An immittance converter (IC), an abbreviation of impedance-admittance converter, is a two-port network, in which the input impedance is proportional to the load admittance connected across the output terminals [6]. In an IC, the output current is proportional to the input voltage and the output voltage is proportional to the input current. This characteristic feature of an IC enables the conversion of a constant voltage (CV) source to constant current (CC) source and vice versa, which is useful in many power electronics applications.

The immittance conversion characteristics (ICC) of a quarter-wave distributed constant line has been explored in the past for lamp ballasts [7], induction heating [8], and corona and plasma discharge applications [9]-[11] operating in the megahertz-range. Since the length of the distributed constant line becomes prohibitively long for power converters operating in kilohertz-range, some lumped-element IC topologies based on transmission line approximation, emulated using discrete inductors and capacitors, have been studied and reported [6]. However, only two of the reported IC topologies are suitable for power electronics applications, wherein the exciting voltage is commonly a square-wave, which is conveniently obtained by operating power semiconductor switches at a high frequency.

Therefore, a separate class of RCs, referred to as resonant immittance converters (RICs), has been recently reported in [12], in which the resonant network (RN) exhibits ICC. In all, 24 RICs have been identified with three and four reactive elements, out of which 9 topologies (termed Type-I RICs) are suitable for CC to CV conversion and 15 topologies (termed Type-II RICs) are suitable for CV to CC conversion.

LCL-T RC is the simplest of the Type-II RICs. A detailed analysis and design of the LCL-T RC as a constant-current (CC) power supply is reported in [13]. The addition of clamp diodes on the primary side of the converter results in an in-built constant-current – constant-voltage (CC-CV)

Manuscript received Aug. 30, 2011 ; revised Dec. 19, 2011
Recommended for publication by Associate Editor Yong-Chae Jung.
†Corresponding Author: mbb@rrcat.gov.in
Tel: +91-731-2488025, Fax: +91-731-2488000, Raja Ramanna Centre for Advanced Tech.
*Bhabha Atomic Research Centre, India
**Raja Ramanna Centre for Advanced Technology, India

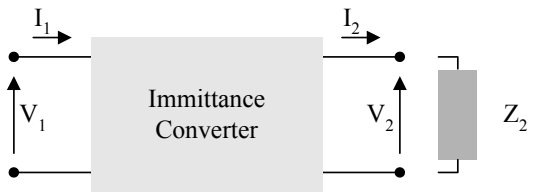

Fig. 1. Two-port immittance converter.

characteristic [14] making the converter suitable for capacitor charging applications [15]. The presence of a transformer winding capacitance changes the LCL-T RC into a fourth-order LC-LC topology, which has been shown to behave as a Type-II RIC [16]. The various modes of operation and issues in the design of a LCL-T RC with asymmetrical duty-cycle control are described in [17]. LCL-T RC topologies are also reported for various applications such as radio frequency inductive discharges [18], inverters for photovoltaic systems [19] and non-contact energy transmission systems [20]. The application of a Type-I RIC (CLC- π network) in a high-voltage dc transmission link is reported in [21]. The characteristics of a five-element RIC topology are studied in [22]. The analysis and design of a five-element T-type Type-II RIC topology has been reported in [23].

The ability of a Type-II RIC to convert a voltage source into a current source is very useful in a variety of applications wherein a CC source is either inherently required or can be advantageously applied. These application areas include capacitor charging power supplies, battery chargers, laser diode drivers, power supplies for electromagnets, power supplies for electro-chemical processes, high voltage power supplies, CC and CC-CV power supplies for electric arc welding, illumination systems, etc.

While a methodology for the steady-state analysis and design of RICs is well established and demonstrated [12] – [23], transient and small-signal analysis have not been reported. The dynamic response of a converter during transients must be considered while formulating its design procedure. Similarly, small-signal analysis is necessary to derive various transfer functions and to design the feedback controller.

Various methods have been reported in the literature [24]-[30] for the transient and small-signal analysis of RCs. These methods can also be applied to RICs since they are a special type of RCs. However, the objective of this paper is to propose a simpler and approximate equivalent circuit model of the Type-II RIC family that predicts the averaged response of the terminal voltages and currents under large-signal variations in the operating conditions. It can be seen that the overall response is dominated by the state variables associated with the output filter, which is therefore particularly important for the controller design. The effect of the state variables associated with the rest of the converter is neglected, which affects only the high frequency response of the converter [24]-[30]. A small-signal model is subsequently derived by applying the perturbation and linearization to the average model.

The derived models greatly simplify and speed-up the analysis either via simple analytical treatment or by using the models in circuit simulation tools. These models are validated by comparing their results with those obtained from cycle-by-cycle simulations and with an experimental prototype.

II. TYPE-II RICS

A block diagram of a two-port IC is shown in Fig. 1, in which the voltages and currents at the input and output ports (represented by V_1, I_1, V_2 and I_2, respectively) are related as given by the following expression:

$$\begin{bmatrix} V_1 \\ I_1 \end{bmatrix} = \begin{bmatrix} 0 & \mp jZ_n \\ \pm j(1/Z_n) & 0 \end{bmatrix} \cdot \begin{bmatrix} V_2 \\ -I_2 \end{bmatrix} \quad (1)$$

where Z_n is the characteristic impedance of the circuit.

An electrical networks composed of lumped reactive elements (inductors and capacitors) exhibiting ICC and having either a low-pass or band-pass frequency response, (consistent with the definition of a RC) has been termed a resonant immittance network (RIN) [12]. When a RIN is used in place of an ordinary RN in a RC, the resulting power converter topology

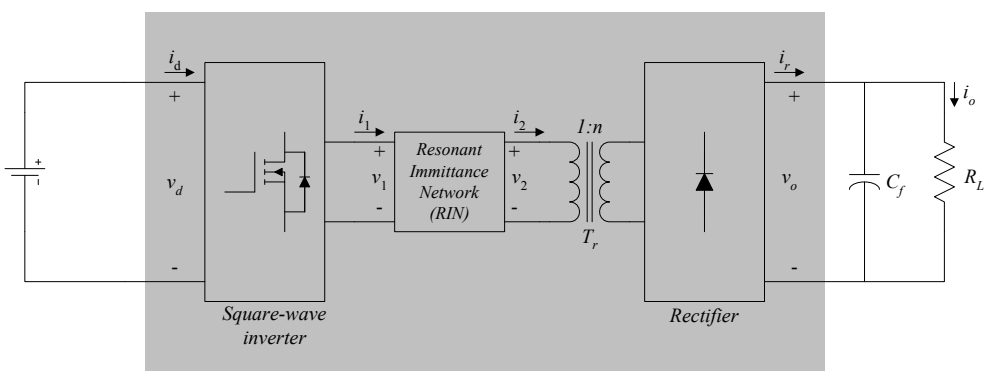

Fig. 2. Block diagram of dc-dc Type-II RIC.

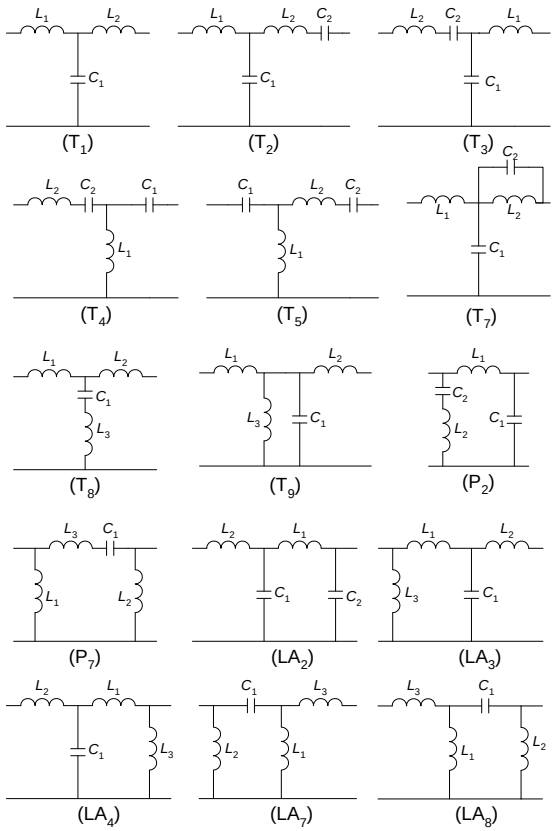

Fig. 3. Three- and Four-element Type-II RINs [12].

is termed a RIC. A generic block diagram for a voltage-source or Type-II dc-dc RIC can be drawn as shown in Fig. 2. An inverter (full-bridge, half-bridge or push-pull) excites the Type-II RIN with a high frequency square-wave voltage waveform. Figure 3 summarizes the 15 Type-II RINs, with three and four reactive elements, reported in [12]. In the nomenclature, T stands for T-type RIN, P stands for π-type RIN and LA stands for ladder-type RIN. A transformer at the output of a RIN is used to step-up or down the voltage according to the requirements and to provide galvanic isolation. A rectifier and filter are used to get the dc output.

RICs exhibit ICC only if various reactances obey certain conditions, which are satisfied only at a particular frequency of operation and when the values of the reactive elements are suitably chosen [12]. These circuits have different properties at other frequencies. Therefore, as opposed to other RCs, RICs can not be controlled by varying the switching frequency or else the ICC will be lost. Due to the low-pass or band pass characteristics of a RIN, the current at its input and output port is nearly sinusoidal. Further, due to the ICC, v_1 and i_1 are always in phase under all loading conditions. Assuming a large output filter capacitor, and therefore ripple free output voltage, the voltage at the output port of the RIN, v_2, has a square-wave waveform with an amplitude of ($\pm v_o/n$). Furthermore, it is in phase with i_2 due to the rectifier action. It can be seen from (1)

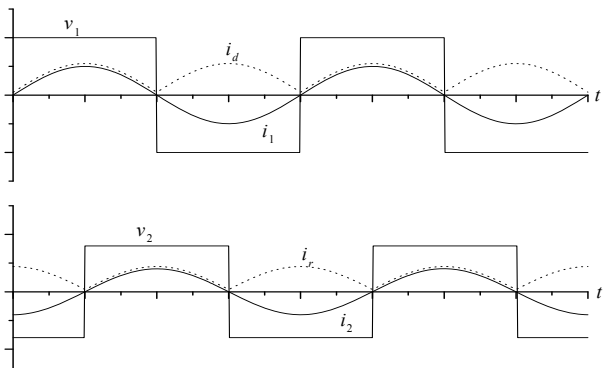

Fig. 4. Idealized waveforms of dc-dc Type-II RIC.

that the phase difference between v_1 and v_2 as well as that between i_1 and i_2 will be 90°. Therefore, the idealized voltage and current waveforms at the input and output port of the RIN can be drawn, as shown in Fig. 4. The figure also shows the waveforms of the rectified output current, i_r, and the current drawn from the input dc source, i_d.

III. Approximate Equivalent Circuit Model of Type-II RICs

The use of equivalent circuits is an intuitive approach which allows the well-known techniques of circuit analysis to be employed. Averaging has been one of the most important tools for power converter design and analysis since it adequately describes the functional relationships between sources, outputs and control parameters, while ignoring ripple.

A. Approximate Equivalent Circuit Model of Type-II RINs

The RIN shown in the block diagram of Fig. 2 can be any of the three- and four-element networks, shown in Fig. 3, for a Type-II RIC.

To study the small-signal behavior of Type-II RINs, the envelop simulation method using the SPICE-compatible models developed in [29], [30] is used. The designed component values in the experimental prototypes of topology T_1 in [13], [14], [17], topology LA_2 in [16] and topology T_3 in [12] are used to obtain the input voltage-to-output current transfer functions from the simulation. The component values used for the simulation are summarized in table 1. Since only the small-signal behavior of a RIN is being investigated, the transformer, rectifier, filter and load resistance connected at the output port of the RIN are replaced by an equivalent ac resistance (R_{ac}) whose value corresponds to the rated maximum load resistance in the respective prototype. This is also mentioned in table 1. Figure 5 shows the gain and the phase response of the input voltage-to-output current transfer functions in these circuits. It can clearly be seen from the plots of Fig. 5 that the low-frequency response of these converters is

TABLE I

DESIGNED VALUES OF COMPONENT IN VARIOUS RINS

	T_1 [13]	T_1 [14]	T_1 [17]	LA_2 [16]	T_3 [12]
L_1 (μH)	16.11	25.6	39.18	77.7	48.4
L_2 (μH)	16.11	25.6	39.18	44.63	72.6
C_1 (μF)	0.151	0.1	0.065	0.047	0.047
C_2 (μF)	-	-	-	0.020	0.094
R_{ac} (Ω)	10.13	16.21	16.62	40.52	26.41
f_s (kHz)	100	100	100	83.28	105

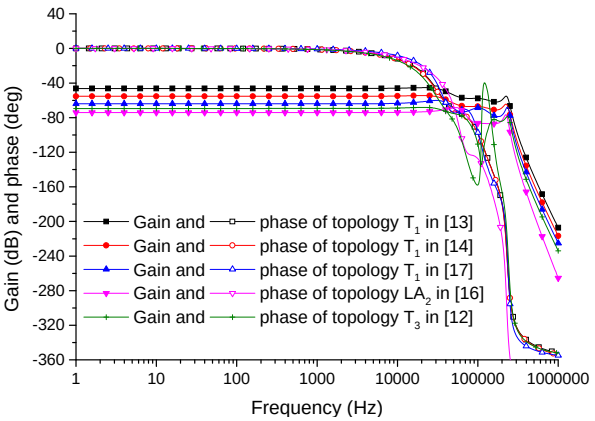

Fig. 5. Small-signal input voltage-to-output current transfer function for topology T_1, LA_2 and T_3 obtained from envelop-simulation method.

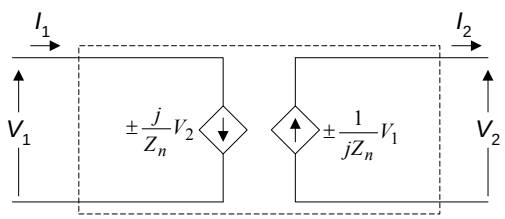

Fig. 6. Approximate equivalent circuit of Type-II RIN.

relatively flat and that the state variables associated with these RINs affect the response only at the high frequencies in the vicinity of the switching frequency. The overall response of a RIC depends on the response of the RIN and its output filter. The output filter in a RIC has a cut-off frequency that is much lower than the switching frequency and it can be expected to dominate the overall low-frequency response, which is particularly important for the controller design. Therefore, neglecting the high-frequency behavior of a Type-II RIN, the relationship between the voltages and currents at its input and output ports [given by (1)], can be represented by the equivalent circuit shown in Fig. 6. Note that this equivalent circuit model is valid for Type-II RICs operating at a fixed frequency where RIN exhibits ICC.

B. Approximate Equivalent Circuit Model of Type-II RICs

While a Type-II RIN, can be represented by the equivalent circuit in Fig. 6, the nonlinear elements of a RIC (the inverter and rectifier at the input and output side, respectively) do not directly allow a simpler equivalent circuit representation of a complete RIC. If the shaded portion of the block diagram in Fig. 2 can be represented using an equivalent circuit describing the terminal relationship in terms of the average values of v_d, i_d and v_o, i_r, the task of the circuit analysis would greatly be simplified since the rest of the circuit elements are linear.

The average values of i_d and i_r are given by:

$$\langle i_d(t)\rangle_{T_s} = \frac{2\sqrt{2}I_1}{\pi}, \quad \langle i_r(t)\rangle_{T_s} = \frac{2\sqrt{2}I_2}{n\pi} \tag{2}$$

where $\langle x(t)\rangle_{T_s}$ denotes the average of $x(t)$ over an interval of one period T_s:

$$\langle x(t)\rangle_{T_s} = \frac{1}{T_s}\int_{t}^{t+T_s} x(\tau)d\tau \tag{3}$$

I_1 and I_2 are the rms values of i_1 and i_2, respectively. Similarly, the rms values of the fundamental components of v_1 and v_2 (V_1 and V_2, respectively) are given in terms of the dc input and output voltage (V_d and V_o, respectively) as:

$$V_1 = \frac{2\sqrt{2}\langle v_d(t)\rangle_{T_s}}{\pi}, \quad V_2 = \frac{2\sqrt{2}\langle v_o(t)\rangle_{T_s}}{n\pi} \tag{4}$$

By substituting (2) and (4) into (1) and neglecting the phasor terms for the dc quantities, the following is obtained:

$$\begin{bmatrix}\langle v_d(t)\rangle_{T_s}\\ \langle i_d(t)\rangle_{T_s}\end{bmatrix} = \begin{bmatrix}0 & \rho\\ \rho^{-1} & 0\end{bmatrix}\cdot\begin{bmatrix}\langle v_o(t)\rangle_{T_s}\\ \langle i_r(t)\rangle_{T_s}\end{bmatrix} \tag{5}$$

where:

$$\rho = \frac{\pi^2}{8}nZ_n \tag{6}$$

Thus the shaded portion of Fig. 2, whose terminal voltages and currents are described by (5), can be represented by the equivalent circuit shown in Fig. 7(a). By connecting the source and load at the input and output terminals of the equivalent circuit, an equivalent circuit model of a Type-II RIC can be constructed, as shown in Fig. 7(b). This equivalent circuit model can be easily analyzed using classical circuit theory to determine the steady-state characteristics as well as the transient response to track averaged large-scale changes in the terminal voltages and currents as the source or load undergo changes. Alternatively, the equivalent circuit can be directly simulated with various circuit simulation tools to directly obtain the averaged terminal response.

IV. SMALL-SIGNAL AC MODEL

To construct a small signal ac model at a quiescent operating point it is assumed that the input voltage is equal to some given quiescent value V_d plus some superimposed small

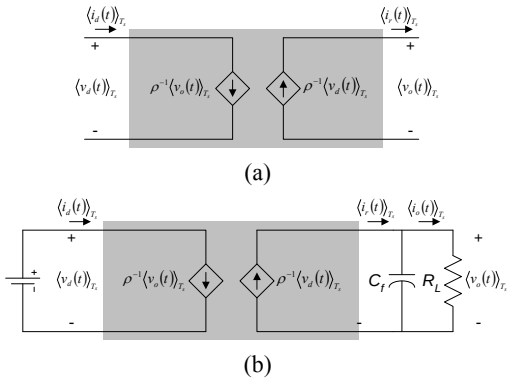

Fig. 7. Equivalent circuit model of (a) shaded portion of the block diagram of Fig. 2, and (b) Type-II RIC.

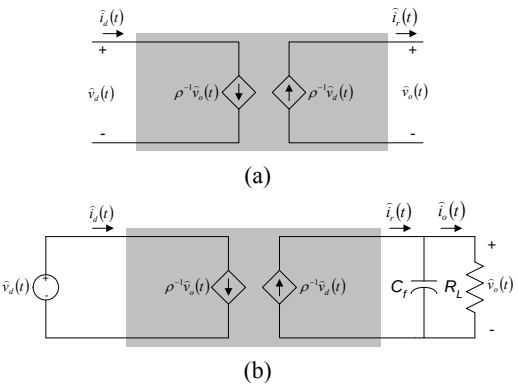

Fig. 8. Small-signal ac equivalent circuit model of (a) shaded portion of the block diagram of Fig. 2, and (b) Type-II RIC.

ac variation $\hat{v}_d(t)$. As a result, the following is obtained:

$$\langle v_d(t)\rangle_{T_s} = V_d + \hat{v}_d(t) \tag{7}$$

In response to this input, after the transients have subsided, the averaged input current $\langle i_d(t)\rangle_{T_s}$, the averaged rectified output current $\langle i_r(t)\rangle_{T_s}$ and the averaged output voltage $\langle v_o(t)\rangle_{T_s}$ will be equal to the corresponding quiescent values I_d, I_r and V_o, plus some superimposed small ac variations, $\hat{i}_d(t)$, $\hat{i}_r(t)$ and $\hat{v}_0(t)$, respectively. As a result, the following is obtained:

$$\langle i_d(t)\rangle_{T_s} = I_d + \hat{i}_d(t) \tag{8}$$

$$\langle i_r(t)\rangle_{T_s} = I_r + \hat{i}_r(t) \tag{9}$$

$$\langle v_o(t)\rangle_{T_s} = V_o + \hat{v}_o(t) \tag{10}$$

Substituting (7) – (10) into (5) and simplifying, the following is obtained:

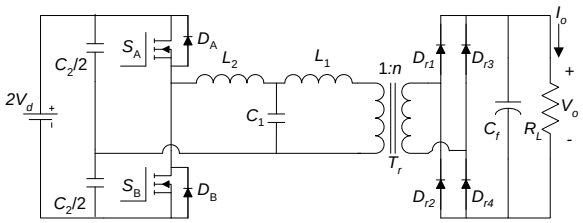

Fig. 9. Circuit diagram of half-bridge T_3 RIC [12].

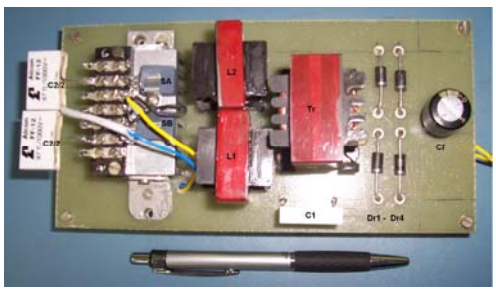

Fig. 10. Photograph of the experimental prototype of T_3 RIC.

$$\begin{bmatrix}\hat{v}_d(t)\\ \hat{i}_d(t)\end{bmatrix} = \begin{bmatrix}0 & \rho\\ \rho^{-1} & 0\end{bmatrix}\cdot\begin{bmatrix}\hat{v}_o(t)\\ \hat{i}_r(t)\end{bmatrix} \tag{11}$$

This relationship in the small-signal quantities, being similar to (5), can be represented by a similar equivalent circuit, as shown in Fig. 8. Subsequently, the line-to-output transfer functions and the input impedance of a Type-II RIC can be readily derived as:

$$G_1(s) = \frac{\hat{i}_o(s)}{\hat{v}_d(s)} = \frac{1}{\rho}\frac{1}{1+sR_LC_f} \tag{12}$$

$$G_2(s) = \frac{\hat{v}_o(s)}{\hat{v}_d(s)} = \frac{R_L}{\rho}\frac{1}{1+sR_LC_f} \tag{13}$$

$$Z_{in}(s) = \frac{\hat{v}_d(s)}{\hat{i}_d(s)} = \frac{\rho^2}{R_L}\left(1+sR_LC_f\right) \tag{14}$$

V. Simulation and Experimental Results

The equivalent circuit models in Fig. 7 and Fig. 8 can be easily analyzed to determine the steady-state characteristics, the transient response to track the averaged large-scale changes in the terminal voltages and currents as the source or load undergoes a change, the derivation of the small-signal transfer function and the visualization of the frequency response. Alternatively, the equivalent circuit can be directly simulated with various circuit simulation tools.

To validate the models, they are implemented in OrCad PSpice and the results are compared with those obtained from a cycle-by-cycle simulation as well as an experimental prototype of the newly identified RIC topology T_3 [12]. Fig. 9 shows the circuit diagram of a half-bridge T_3 RIC. The converter operates with 220 V of dc input and provides 1 A of dc output current with a maximum load resistance of 250 Ω. The values of the reactive components of the RIN are already listed in table 1.

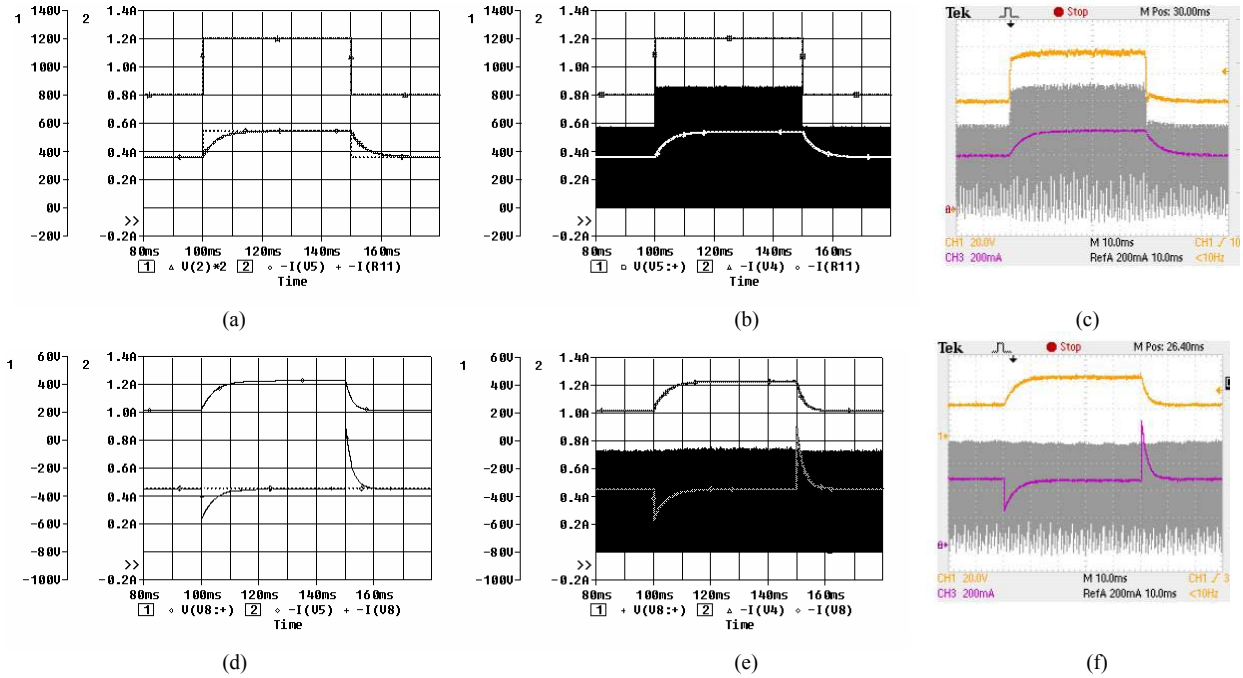

Fig. 11. Response of Topology T_3 to step change in input dc voltage [(a), (b), (c)] and step change in R_L. [(d), (e), (f)]. (a), (d): Predicted average response from the equivalent circuit model. [Top trace: $\langle v_d \rangle_{T_s}$, dotted trace: $\langle i_r \rangle_{T_s}$ and continuous trace: $\langle i_o \rangle_{T_s}$]. (b), (e): Results of cycle-by-cycle simulation. (c), (f): Experimental results. In parts (b) and (c), the waveform at the top shows $v_d(t)$, the envelop shows $i_r(t)$ and the trace the bottom shows $i_o(t)$.

The transformer turns ratio is 1:2.77 (a 9-turn primary and a 25-turn secondary on an EE 42.21.20 ferrite core). Fig. 10 shows a photograph of the experimental setup which is operated in the open loop to check the open-loop transient response and the small-signal transfer function.

The filter capacitor C_f is 47 μF. When $Z_n \left(\equiv \sqrt{L_1/C_1}\right)$= 32.09 and n = 2.77, ρ is calculated from (6) to be 109.66. Fig. 11(a), (b) and (c) shows the response of the converter operating with R_L = 94 Ω, when the input dc voltage ($2V_d$) undergoes a step change from 80 V to 120 V and vice versa. Similarly, Fig. 11(d), (e) and (f) shows the response of the converter with a step change in R_L from 47 Ω to 94 Ω and vice versa. The following observations are made:

1. The results of the equivalent circuit model are in excellent agreement with those obtained from the cycle-by-cycle simulation and the experiment, thereby confirming the validity of the proposed model.
2. In Fig. 11(a), (b) and (c), the waveform of $i_r(t)$ (or, $\langle i_r \rangle_{T_s}$) instantaneously follows the applied step variation in $v_d(t)$ (or, $\langle v_d \rangle_{T_s}$). However, the response of $i_o(t)$ (or, $\langle i_o \rangle_{T_s}$) is governed by the output filter. Similarly, in Fig. 11(d), (e) and (f), $i_r(t)$ (or, $\langle i_r \rangle_{T_s}$) is constant under the transient condition following the step change in R_L. The waveform of $i_o(t)$ (or, $\langle i_o \rangle_{T_s}$) shows the transient undershoot and overshoot due to an additional current absorbed or delivered by C_f to maintain the charge balance with varying $v_o(t)$ (or, $\langle v_o \rangle_{T_s}$) as R_L varies.

The proposed equivalent circuit model simplifies and speeds up the large signal transient analysis of the converter. Simulation of the model takes a few seconds, which is a huge improvement over the 10s of minutes required for a cycle-by-cycle simulation.

The results in Fig. 12 show that perturbations in $i_r(t)$ (or, $\langle i_r \rangle_{T_s}$) are in phase with the sinusoidal perturbations in $v_d(t)$ (or, $\langle v_d \rangle_{T_s}$) over a wide range of frequencies (1 Hz – 1000 Hz). However, perturbations in $i_o(t)$ (or, $\langle i_o \rangle_{T_s}$) are significantly attenuated and shifted in phase at higher frequencies due to the output filter capacitor.

Finally, the converter's line-to-output small-signal transfer function given by (12), with C_f = 47 μF, R_L = 94 Ω and ρ = 109.66, is found to be in excellent agreement with the experimental observations shown in Fig. 13.

VI. CONCLUSIONS

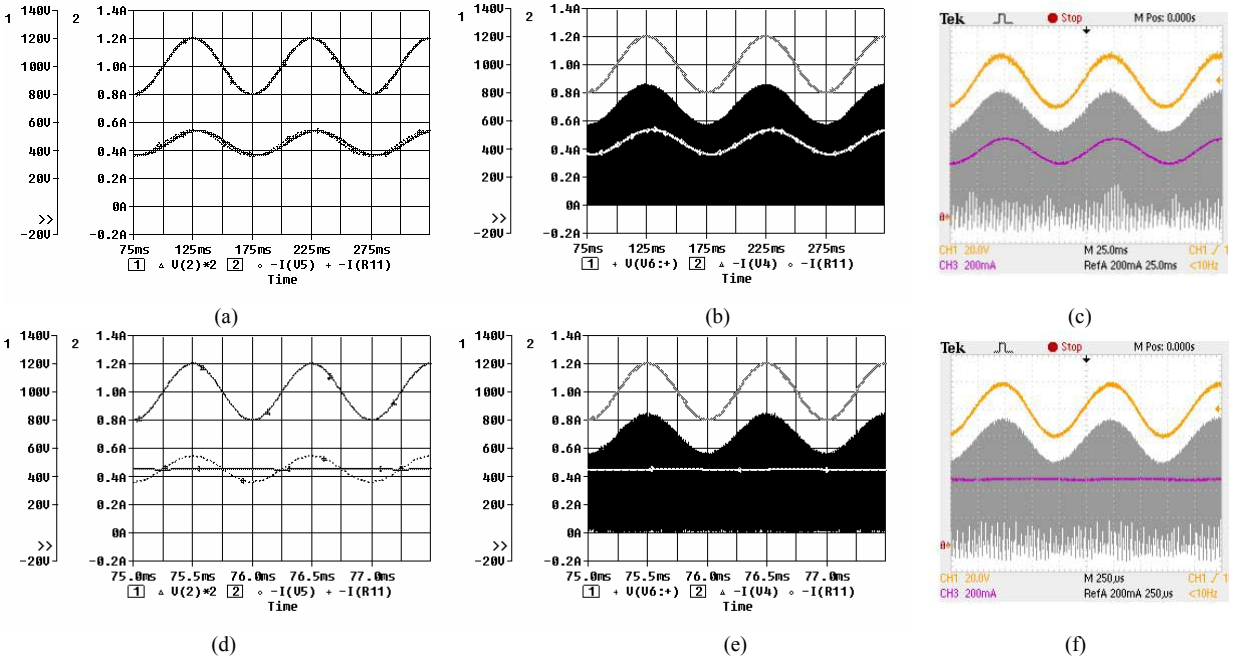

Fig. 12: Response of Topology T_3 to sinusoidal perturbations in dc voltage. (a), (b), (c): 10 Hz, and (d), (e), (f): 1000 Hz.. (a), (d): Predicted response from the proposed model [Top trace: $\langle v_d \rangle_{T_s}$, dotted trace: $\langle i_r \rangle_{T_s}$ and continuous trace: $\langle i_o \rangle_{T_s}$]. (b), (e): The results of cycle-by-cycle simulation. (c), (f): Experimental results. In parts (b) and (c), the waveform at the top shows $v_d(t)$, the envelop shows $i_r(t)$ and the trace the bottom shows $i_o(t)$.

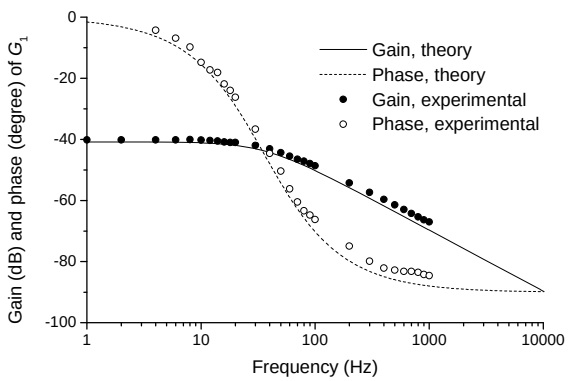

Fig. 13. Theoretical and experimental line-to-output small-signal transfer function of Topology T_3.

RICs are operated at a fixed frequency where the RIN exhibits ICC. Following the envelop simulation method, the small-signal behavior of Type-II RINs is studied and it is observed that the low-frequency response is relatively flat and that the state variables associated with these RINs affect the response only at the high frequencies in the vicinity of the switching frequency. Therefore, an approximate equivalent circuit model and a small-signal model of Type-II RICs, neglecting the high-frequency effect of the state variables associated with RINs, is proposed in this paper. While the proposed models greatly simplify and speed-up the analysis, the open-loop transient and small-signal ac behavior of Type-II RICs is also adequately predicted. The validity of the proposed models is confirmed by comparing their results with those obtained from a cycle-by-cycle simulation and with those of an experimental prototype. It is shown that the low-frequency open-loop transient and small-signal ac behavior of Type-II RICs is governed by only the filter while the converter along with the RIN do not contribute to the low-frequency dynamics.

REFERENCES

[1] J. L. Sosa, M. Castilla, J. Miret, L. Garcia de Vicuna, and J. Matas, "Modeling and performance analysis of the DC/DC series–parallel resonant converter operating with discrete self-sustained phase-shift modulation technique," *IEEE Trans. Ind. Electron.,* Vol. 56, No. 3, pp. 697-705, Mar. 2009.

[2] J. Sun, X. Ding, M. Nakaoka, and H. Takano, "Series resonant ZCS-PFM DC-DC converter with multistage rectified voltage multiplier and dual mode PFM control scheme for medical use high voltage x-ray power generator," *IEE Proc. Electr. Power. Appl.*, Vol. 147, No. 6, pp. 527-534, Nov. 2000.

[3] M. S. Agamy and P. K. Jain, "A three-level resonant single-stage power factor correction converter: analysis, design, and implementation," *IEEE Trans. Ind. Electron.*, Vol. 56, No. 6, pp. 2095-2107, Jun. 2009.

[4] H. Suryawanshi, V. Borghate, M. Ramteke, and K. Thakre, "Electronic ballast using a symmetrical half-bridge inverter operating at unity-power-factor and high efficiency," *Journal of Power Electronics,* Vol. 6, No. 4, pp.330-339, Oct. 2006.

[5] H. Sugimura, H. Muraoka, T. Ahmed, S. Chandhaket, E. Hiraki, M. Nakaoka, and H. Lee, "Dual mode phase-shifted

zvs-pwm series load resonant high-frequency inverter for induction heating super heated steamer," *Journal of Power Electronics,* Vol. 4, No. 3, pp.138-151, Jul. 2004.
[6] H. Irie and H. Yamana, "Immittance converter suitable for power electronics," *Trans. of I.E.E. Japan*, Vol. 117D, No. 8, pp. 962-969, 1997.
[7] H. Ohguchi, M. H. Ohsato, T. Shimizu, G. Kimura, and H. Takagi, "A high-frequency electronic ballast for HID lamp based on a λ/4-long distributed constant line," *IEEE Trans. Power Electron.*, Vol. 13, No. 6, pp. 1023-1029, Nov. 1998.
[8] T. Shimizu and M. Shioya, "Characteristics of electric power transmission on high-frequency inverter having distributed constant line," *IEEE Trans. Ind. Electron.*, Vol. 38, No. 2, pp. 115-120, Apr. 1991.
[9] H. Ohguchi, M. Tamate, R. Shimotaya, H. Takagi, and M. Ito, "13.56 MHz current source generator based on third harmonic power transmission using immittance conversion topology and investigation on novel immittance conversion element," *Proc. IEEE ISIE*, pp. 477-481, 2000.
[10] T. Shimizu, H. Kinjyo, and K. Wada, "A novel high-frequency current output inverter based on an immittance conversion element and a hybrid MOSFET-SIC diode switch," Proc. IEEE PESC, pp. 2003-2008, 2003.
[11] Y. Sakamoto, K. Wada, and T. Shimizu, "A 13.565 MHz current-output-type inverter utilizing an immittance conversion elemet," *Proc of Int. Power Electronics and Motion Control Conference (EPE- PEMC)*, pp. 288-294, 2008.
[12] M. Borage, K. V. Nagesh, M. S. Bhatia, and S. Tiwari, "Resonant immittance converter topologies," *IEEE Trans. Ind. Electron*., Vol. 58, No. 3, pp. 971-978, Mar. 2011.
[13] M. Borage, S. Tiwari, and S. Kotaiah, "Analysis and design of LCL-T resonant converter as a constant-current power supply," *IEEE Trans. Ind. Electron.,* Vol. 52, No. 6, pp. 1547-1554, Dec. 2005.
[14] M. Borage, S. Tiwari, and S. Kotaiah, "LCL-T resonant converter with clamp diodes: A novel constant-current power supply with inherent constant-voltage limit," *IEEE Trans. Ind. Electron.*, Vol. 54, No. 2, pp. 741-746, Apr. 2007.
[15] M. Borage, S. Tiwari, and S. Kotaiah, "A constant-current, constant-voltage half-bridge resonant power supply for capacitor charging," *IEE Proc. Electr. Power. Appl.*, Vol. 153, No. 3, pp. 343-347, May 2006.
[16] M. Borage, K. V. Nagesh, M. S. Bhatia, and S. Tiwari, "Design of LCL-T resonant converter including the effect of transformer winding capacitance," *IEEE Trans. Ind. Electron*, Vol. 56, No. 5, pp. 1420-1427, May 2009.
[17] M. Borage, K. V. Nagesh, M. S. Bhatia, and S. Tiwari, "Characteristics and design of an asymmetrical duty-cycle controlled LCL-T resonant converter," *IEEE Trans. Power Electron,* Vol. 24, No. 10, pp. 2268-2275, Oct. 2009.
[18] M. A. Razzak, S. Takamura, Y. Uesugi, and N. Ohno, "Efficient radio frequency inductive discharge in near atmospheric pressure using immittance conversion topology," *Journal of Plasma and Fusion Research*, Vol. 81, No. 3, pp. 204-211, Mar. 2005.
[19] E. Zhang, "Inverter design shiens in photovoltaic systems," *Power Electronics Technology*, pp. 20-25, Jul. 2008.
[20] H. Irie, N. Minami, H. Minami, and H. Kitayoshi, "Non-contact energy transfer system using immittance converter," *Electrical Engineering in Japan*, Vol. 136, No. 4, pp. 58-64, Jul. 2001.
[21] N. Kimura, K. Tanaka, T. Morizane, and K. Taniguchi, "Analysis of HVDC converter with immittance conversion link," *Proc. EPE*, pp. P.1-P., 1999.
[22] M. Tamate, H. Ohguchi, M. Hayashi, H. Takagi, and M. Ito, "A novel approach of power converter topology based on immittance conversion theory," *Proc. IEEE ISIE*, pp. 482-487, 2000.
[23] M Borage, K. V. Nagesh, M. S. Bhatia and S. Tiwari, "Analysis and design is higher-order t-type resonant convertor as a constant current power supply," *IET Transactions on Power Electronics* Vol. 4, No. 1, pp. 72-80, Jan. 2011.
[24] V. Vorperian and S. Cuk, "Small signal analysis of resonant converters," *IEEE Power Electronics Specialist Conference Proc*, pp. 265-278, 1983.
[25] V. Vorperian, "Approximate small signal analysis of series and parallel resonant converters," *IEEE Trans. Power Electron.*, Vol. 4, No. 1, pp. 15-24, Jan. 1989.
[26] A. Witulski, A. Hernandez, and R. Erickson, "Small signal equivalent circuit modeling of resonant converters," *IEEE Trans. Power Electron.*, Vol. 6, No. 1, pp. 11-27, Jan. 1991.
[27] I. Batarseh and K. Siri, "Genaralized approach to the small signal modeling of DC-DC resonant converters," *IEEE Trans. Aerosp. Electron. Syst.*, Vol. 29, No. 3, pp. 894-908, Jul. 1993.
[28] S. Ben-Yaakov and G. Rahav, "Average modeling and simulation of series-parallel resonant converters by SPICE compatible behavioral models," *IEEE Applied Power Electronics Conference Proc.*, pp. 116-120, 1996.
[29] Y. Yin, R. Zane, J. Glaser, and R. W. Erickson, "Small-signal analysis of frequency-controlled electronic ballasts," *IEEE Trans. Circuits Syst. I, Fundam. Theory Appl.*, Vol. 50, No. 8, pp. 1103-1110, Aug. 2003.
[30] S. Lineykin and S. Ben-Yaakov, "Unified SPICE-compatible model for large and small-signal envelop simulation of linear circuits excited by modulated signals," *IEEE Trans. Ind. Electron.*, Vol. 53, No. 3, pp. 745-751, Jun. 2006.

Mangesh Borage received his B.E. in Electrical Engineering from Shivaji University, Kolhapur, India, in 1993. He received his M.Tech. also in Electrical Engineering, with a specialization in Power Electronics, from the Banaras Hindu University, Varanasi, India, in 1996. He joined the 38th batch of training school at the Bhabha Atomic Research Centre (BARC), Mumbai, India, in 1994. Since 1995, he has been with the Raja Ramanna Centre for Advanced Technology (RRCAT), Indore, India. His research interests include soft-switching and resonant converters, power factor correction, high-frequency magnetic components and high-frequency power converters. Mr. Borage is a recipient of University Merit Certificate from Shivaji University, Kolhapur, India, for First Rank in Electrical Engineering, in 1993. He is also a recipient of Dr. Homi Bhabha Award at BARC, Mumbai, India, in 1995.

K. V. Nagesh received his B.E. in Electrical Power and his M.E. in Power System Engineering from the University of Mysore, Karnataka, India, in 1972 and 1974, respectively. He received his Ph.D. from the High Voltage Engineering Department at the Indian Institute of Science, Bangalore, in 1998. He was with the Bhabha Atomic Research Centre, Mumbai, India, from 1975 to 2011, where he was associated with the development of various pulse power systems.

M. S. Bhatia was born in New Delhi, India on 6th October, 1954. He received his B.E. in Electrical Engineering from the Delhi College of Engineering, Delhi, India, in 1977. He received his Ph.D. from the Indian Institute of Technology Delhi (IIT Delhi), New Delhi, India, in 1993. He is currently heading the Beam Electronics and Application Section of the Bhabha Atomic Research Centre, Mumbai, India. His research interests include electron beam technology, lasers and plasma devices.

Sunil Tiwari received his B.E. in Electronics Engineering from Maharaja Sayajirao University, Vadodra, India, in 1984. He was with Bharat Heavy Electricals Limited (BHEL), Bangalore, India, from 1984 to 1987 and with the Ministry of Defence, Agra, India, from 1987 to 1989. Since 1989 he has been with the Raja Ramanna Centre for Advanced Technology (RRCAT), Indore, India, as a Scientific Officer. His research interests include soft-switching and resonant techniques for high power applications and the development of high stability power supplies for particle accelerators.